Cellular/Molecular

Regulation of Axonal Elongation and Pathfinding from the Entorhinal Cortex to the Dentate Gyrus in the Hippocampus by the Chemokine Stromal Cell-Derived Factor 1α

Yoichi Ohshima,[1,2,3] Takekazu Kubo,[2] Ryuta Koyama,[4] Masaki Ueno,[1,2] Masanori Nakagawa,[3] and Toshihide Yamashita[1,2]

[1]Department of Molecular Neuroscience, Graduate School of Medicine, Osaka University, Osaka 565-0871, Japan, [2]Department of Neurobiology, Graduate School of Medicine, Chiba University, Chiba 260-8670, Japan, [3]Molecular Neurology and Gerontology, Kyoto Prefectural University of Medicine, Kyoto 602-8566, Japan, and [4]Laboratory of Chemical Pharmacology, Graduate School of Pharmaceutical Sciences, The University of Tokyo, Tokyo 113-0033, Japan

During the early developmental stage, a neural circuit is established between the entorhinal cortex (EC) and the hippocampal dentate gyrus (DG) via the perforant pathway. However, the manner in which the perforant fibers are navigated has mostly remained a mystery. Here, we analyzed the functional role of a chemokine, namely, stromal cell-derived factor 1α (SDF-1α), in the navigation of the perforant fibers. SDF-1α was observed to promote neurite growth, which is dependent on mDia1, in cultured entorhinal cortical neurons obtained from rats at postnatal day 0. We then used entorhino-hippocampal cocultures comprising green fluorescence-labeled EC and DG slices to assess the projection of the perforant fibers from the EC. Although the specific laminar termination of the entorhinal axons was observed with this system, the number of appropriately terminating entorhinal axons decreased significantly when the SDF-1α signaling pathway was blocked by a neutralizing antibody against SDF-1α or by the specific SDF-1α receptor antagonist AMD3100 (1,1′-[1,4-phenylenebis(methylene)]bis-1,4,8,11-tetra-azacyclotetradecane octahydrochloride). Furthermore, inhibition of the SDF-1α signaling pathway resulted in a decrease in the immunoreactivity for PSD-95 (postsynaptic density protein-95) in the DG, possibly because of a reduction in the number of projecting perforant fibers. These results demonstrate that SDF-1α plays a critical role in promoting the growth of perforant fibers from the EC to the DG.

Key words: **stromal cell-derived factor-1; CXCR4; hippocampus; dentate gyrus; entorhinal cortex; axonal elongation; slice culture; cell culture**

Introduction

The entorhino-hippocampal circuitry comprises neurons originating in the entorhinal cortex (EC) and functions as the major excitatory input to both the ipsilateral and contralateral hippocampus/dentate gyrus (DG). This fiber tract comprises projections of the alveolar and perforant pathways and a commissural projection (Skutella and Nitsch, 2001). The perforant fiber extends from the EC to the DG. The afferent pathway arising from EC layer II is one of the major inputs in the DG. Recent studies have provided evidence of the involvement of various membrane-associated attractive or repulsive axon guidance molecules in hippocampal development. For example, the secreted semaphorins and their binding partners, neuropilins, regulate the development of hippocampal fiber projections (Chen et al., 2000; Gu et al., 2003). Plexins are receptors implicated in mediating semaphorin signaling and regulating the development of hippocampal axonal projections (Cheng et al., 2001). Other molecules, including ephrins (Stein et al., 1999), netrins (Steup et al., 2000), Slits (Nguyen Ba-Charvet et al., 1999), and ECM (extracellular matrix) molecules (Zhao et al., 2003), have been reported to regulate the development of hippocampal circuitry. Although it has been demonstrated that the repulsive guidance molecule a (RGMa) repels the perforant fibers causing them to terminate at the outer molecular layer of the DG (Brinks et al., 2004), the factors inducing the elongation of the perforant fibers from the EC to the DG remain to be elucidated.

Stromal cell-derived factor 1α (SDF-1α) is a chemokine that plays an important role in blood formation (Ara et al., 2005). CXCR4, an SDF-1 receptor, mediates the migration of leukocytes and hematopoietic progenitors (Zou et al., 1998). CXCR4 is known to function as a receptor for HIV-1 (type 1 human immunodeficiency virus) in host cells and is an indispensable molecule for the appearance of AIDS (acquired immunodeficiency syndrome) (Bleul et al., 1997). In the neuronal system, SDF-1α and CXCR4 regulate neural migration and axonal pathfinding (Lieberam et al., 2005; Stumm and Höllt, 2007) and play a critical role in the migration of cerebellar granule neurons during the early developmental stages (Ma et al., 1998; Vilz et al., 2005).

Received Dec. 23, 2007; revised June 24, 2008; accepted June 30, 2008.

This work was supported by National Institute of Biomedical Innovation Research Grant 05-12 and a Grant-in-Aid for Young Scientists (S) from Japan Society for the Promotion of Science (T.Y.).

Correspondence should be addressed to either of the following: Toshihide Yamashita or Takekazu Kubo, Department of Molecular Neuroscience, Graduate School of Medicine, Osaka University, 2-2 Yamadaoka, Suita, Osaka 565-0871, Japan. E-mail: yamashita@molneu.med.osaka-u.ac.jp or kubo@restaff.chiba-u.jp.

DOI:10.1523/JNEUROSCI.1670-08.2008

 0270-6474/08/288344-10$15.00/0

SDF-1–CXCR4 signaling regulates the migration of sensory neuron progenitors to the dorsal root ganglion (Belmadani et al., 2005). Furthermore, it has been demonstrated that the migration of hippocampal dentate granule cells from the ventricular zone to the hippocampus is inhibited in *CXCR4*-knock-out mice (Bagri et al., 2002; Lu et al., 2002). SDF-1α signaling is also required for normal cortical development (Paredes et al., 2006; Li et al., 2008). Moreover, SDF-1α has been shown to enhance the axonal branching of hippocampal neurons derived from rats at postnatal day 18 (Pujol et al., 2005). These data demonstrate that the signaling pathway involving SDF-1α and CXCR4 plays an essential role in neuronal development. In the present study, we assessed the possible involvement of SDF-1α and its receptor in the navigation of perforant fibers from the EC to the DG. To test this hypothesis, we used rat entorhino-hippocampal slice cultures because mice with *SDF-1* or *CXCR4* gene deletions were not an ideal model for our experiments. *CXCR4*-knock-out mice exhibit a defect in the structure of the dentate granule cell layer because of poor migration of the granule cells (Bagri et al., 2002; Lu et al., 2002). By performing a series of experiments, we observed that SDF-1α was involved in the elongation of the perforant fiber from the EC to the DG in the slice culture system.

Materials and Methods

Reagents. The rabbit anti-SDF-1 (1:200) and anti-CXCR4 (SDF-1 receptor; 1:200 for the immunohistochemistry and 1:1000 for Western blot analysis) antibodies were obtained from Torrey Pines Biolabs. The rabbit anti-Rho-associated kinase α (ROKα) antibody (1:500) was obtained from Millipore. The mouse anti-neuronal nuclear (NeuN) monoclonal antibody (1:500) was obtained from Millipore Bioscience Research Reagents. Goat anti-mouse or -rabbit IgG (H+L) conjugated to Alexa Fluor 488 (1:400 for the slice culture and 1:1000 for the dissociated culture) or Alexa Fluor 568 (1:400 for the slice culture and 1:1000 for the dissociated culture) or Alexa Fluor 405 (1:400 for the slice culture) was procured from Invitrogen. Recombinant mouse CXCL12/SDF-1α and the anti-human/mouse CXCL12/SDF-1 antibody were obtained from R&D Systems. 1,1′-[1,4-Phenylenebis(methylene)]bis-1,4,8,11-tetra-azacyclotetradecane octahydrochloride (AMD3100 octahydrochloride hydrate), a specific SDF-1-receptor antagonist, was obtained from Sigma-Aldrich. Polyclonal anti-RGMa antibodies (1:100) were produced in our laboratory (Hata et al., 2006) and obtained from Immunobiological Laboratories. The rat mDia1 short interfering RNA (siRNA) (GeneID 307483) and the control siRNA 1 were obtained from Dharmacon Research. The control siRNA 2 was obtained from Sigma-Aldrich (SiPerfect Negative Control). The mouse mDia1 antibody (1:500) was obtained from BD Biosciences. (*R*)-(+)-*trans*-*N*-(4-pyridyl)-4-(1-aminoethyl)-cyclohexanecarboxamide, 2HCl (Y-27632) was obtained from Calbiochem. The neuronal class III β-tubulin (Tuj1) mouse monoclonal antibody (1:1000) was obtained from Covance. The rabbit anti-Prox1 polyclonal antibody (1:1000), used for labeling dentate granule neurons, and the mouse anti-postsynaptic density protein 95 (PSD-95) monoclonal antibody (1:500), used for labeling the postsynaptic membrane, were procured from Millipore Bioscience Research Reagents. The rabbit polyclonal anti-green fluorescent protein (GFP) antibody (1:500) was obtained from Abcam. 1,1′-Dioctadecyl-3,3,3′,3′-tetramethylindocarbocyanine perchlorate (DiI) was obtained from Invitrogen.

Immunohistochemistry. Brain cryosections (thickness, 10 μm) of rats at postnatal day 0 were prepared. The primary antibodies used were rabbit anti-SDF-1 (1:200), rabbit anti-CXCR4 (1:200), and mouse anti-NeuN (1:500) antibodies. The secondary antibodies used were goat anti-mouse or -rabbit IgG conjugated with Alexa Fluor 488 (1:1000) or Alexa Fluor 568 (1:1000). The sections were treated with 5% bovine serum albumin (BSA) and 0.1% Triton X-100 in PBS for 30 min. After the sections were washed three times in PBS, they were allowed to react with the primary antibodies overnight at 4°C. The sections were washed three times and allowed to react with the secondary antibodies for 1 h at room temperature. They were then observed under a fluorescence microscope (Eclipse E600; Nikon).

In situ *hybridization.* The SDF-1α antisense and the sense riboprobes were generated by transcription of a mouse CXCR4 reading frame region cloned into a pCMV-SPORT 6 (Invitrogen; MGC clone 2864967). The brains of the rats at postnatal day 0 were perfused with 4% paraformaldehyde (PFA) for 2–3 d at 4°C, and then perfused with 30% sucrose/PFA until they sank. The brains were then frozen at −80°C and sectioned at 60 μm on a cryostat. The sections were processed for nonradioactive *in situ* hybridization as described previously (Shimogori et al., 2004).

Cell culture of entorhinal neurons. Entorhinal cortical neurons were obtained from rats at postnatal days 0–1 and were processed as described previously (Hata et al., 2006). The dissociated neurons were plated at 8.0×10^4 cells/cm^2 in slide chambers coated with poly-L-lysine in serum-free DMEM supplemented with B27 (Invitrogen). The neurons were incubated for 1 d in the absence or presence of 400 ng/ml SDF-1α. Where indicated, they were coincubated with 15 μg/ml AMD3100, 60 μg/ml anti-SDF-1 antibody, the anti-RGM antibody (1:100), or 1 μg/ml RGMa. The neurons were also incubated in various concentrations of SDF-1α (10, 25, 100, 400, and 1000 ng/ml) and RGMa (0.2, 1.0, 2.0, and 4.0 μg/ml). The neurons were fixed in 4% PFA for 20 min and blocked for 30 min in PBS containing 5% BSA and 0.1% Triton X-100. Tuj1 was used to label the neurites, and the immunoreactivity was detected by using Alexa Fluor 488-conjugated anti-mouse IgG. The neurons were randomly photographed. Their axon lengths and the number of neurites and branches per neuron were measured. Approximately 50 cells per well and three to four wells per experiment were analyzed.

Knockdown of mDia1. The short interfering double-stranded RNA oligomers (siRNA) for mDia1 (20 μM) or the control siRNAs (20 μM) in nucleofactor solutions (100 μl) was transfected into the entorhinal cortical neurons (1 ml; 4×10^6 cells/ml) using the NucleofectorII Device (Amaxa Biosystems). Then, the cells were plated on 35 mm dishes (for Western blot, at 4.0×10^4/cm^2) or slide chambers (for the neurite growth assay, at 8.0×10^4/cm^2) coated with poly-L-lysine, and incubated in the DMEM including 10% FBS (2×10^5/ml) for 1 or 2 d. Where indicated, the neurons were incubated for a day in the absence or presence of 400 ng/ml SDF-1α and/or 50 μM Y-27632.

Western blot analysis. The neurons were lysed in a lysis buffer containing 50 mM HEPES, 1% NP-40, 5% glycerol, 150 mM NaCl, 10 μg/ml leupeptin, and 10 μg/ml aprotinin. The samples were centrifuged at 15,000 rpm for 5 min, and the supernatant was collected. One-half of the volume of 2× SDS buffer was added to the samples. The mixtures were boiled for 3 min and subjected to SDS-PAGE and Western blot analysis using the anti-mDia1 antibody (1:500), the anti-ROKα antibody (1:500), and the anti-CXCR4 antibody (1:1000).

Slice culture. Neurons obtained from the EC of a GFP transgenic rat (Okabe et al., 1997) or a normal rat and from the hippocampus of a normal rat were used for coculturing (Koyama et al., 2004a). All the brain specimens used were obtained from rats at postnatal days 0–1. The brains were sliced into 300-μm-thick sections on a vibratome (DTK-1000 zero1; Dosaka). The slices were cultured on sterilized culture plate inserts (Millicell) in a minimal essential medium supplemented with 20 mM HEPES buffer and 20% horse serum (Koyama et al., 2004a,b). An entorhinal cortical slice and a hippocampal slice were exactly placed to monitor the projection of the perforant fibers from the EC to the DG (see Figs. 1, 5*A*). The slices were incubated for 9 d in the absence or presence of 50 μg/ml AMD3100, 60 μg/ml anti-SDF-1 antibody, or 10 μg/ml anti-RGM antibody. Furthermore, the slices were fixed in 4% PFA overnight and permeabilized in 0.1 M phosphate buffer (PB) containing 0.4% Triton X-100 overnight. The tissues were blocked for 1 h with 0.1 M PB containing 2% goat serum at room temperature and stained with primary antibodies diluted in 0.1 M PB containing 2% goat serum at 4°C overnight. The primary antibodies used were the mouse anti-NeuN (1:200), rabbit anti-Prox1 (1:1000), anti-GFP (1:500), anti-CXCR4 (1:200), and anti-PSD-95 (1:500) antibodies. The tissues were incubated at 4°C overnight with the secondary antibodies conjugated with Alexa Fluor 568 (1:400), Alexa Fluor 488 (1:400), or Alexa Fluor 680 (1:400). They were then mounted on glass slides and observed under a confocal fluorescence microscope (IX81; Olympus). The GFP fluorescence intensities of the

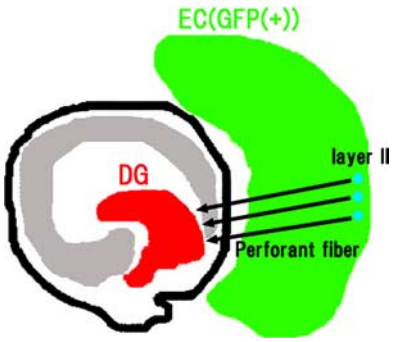

Figure 1. The perforant fibers project from the entorhinal cortex to the dentate gyrus. The perforant fibers emerge from the EC and project to the DG. To analyze the projection of these fibers from the EC to DG, we used rat slice culture systems comprising the EC of a GFP transgenic rat and the hippocampus of rats at postnatal days 0–1. The tissues were sliced to a thickness of 300 μm, and the slices were cocultured for 9 d. The neurons (layer II) in the EC (green) project axons to the DG (arrows).

perforant fibers were measured in eight fields of 25 μm^2 each; the ratios of the intensities of the perforant fibers to the intensities in the EC were calculated, and each value was averaged. Moreover, the fluorescent points labeled with the anti-PSD-95 antibody and/or anti-GFP antibody was counted in five different fields with an area of 100 μm^2 for each sample.

DiI back-labeling of the perforant fibers. The slice tissues were immunostained with the anti-CXCR4 antibody and incubated at 4°C overnight with the secondary antibodies conjugated with Alexa Fluor 405 (1:400). Separately, a glass pin coated with the lipophilic carbocyanine dye, DiI, was placed in the DG in the samples of the slice to label the perforant fibers (see Fig. 8*A*). The samples were incubated for 3–4 d to allow diffusion in 4% PFA at 37°C.

Statistical analysis. One-way ANOVA followed by Scheffé's multiple-comparison test was applied to compare the average values for axon length, fluorescence intensity, or the number of fluorescent points. Values of $p < 0.05$ were considered significant. The statistics repeated from experiment to experiment are used in the experiments using the dissociated cell cultures (see Figs. 3, 4), and the statistics based on the entire cumulative data set are used in the experiments using the slice cultures (see Figs. 5, 7).

Results

SDF-1α is distributed in the DG of the hippocampus, and its receptor, CXCR4, is expressed in the EC

To analyze the navigation of perforant fibers from the EC to the DG, we used rat slice culture systems (Figs. 1, 5*A*). Because *CXCR4*-knock-out mice exhibit a defect in the structure of the dentate granule cell layer as a result of poor migration of the granule cells (Bagri et al., 2002; Lu et al., 2002), we used a previously established explant culture system (Koyama et al., 2004a,b). This system comprises slices of the EC of GFP transgenic rats and the hippocampus of normal rats obtained on postnatal days 0–1. These 300-μm-thick slices were cocultured for 9 d. The navigation of entorhinal axons can be clearly visualized with this culture system.

First, we attempted to assess the possible involvement of SDF-1α in the navigation of entorhinal axons. We examined the distribution of SDF-1α and its receptor, CXCR4, in the hippocampus and EC specimens obtained from rats on postnatal day 0. Axial sections of the hippocampus and EC were immunostained with the anti-SDF-1 or anti-CXCR4 antibody. Intense immunoreactivity for SDF-1 was detected in the dentate granule neurons labeled with the anti-NeuN antibody (Fig. 2*A*,*B*). The signal yielded by SDF-1α disappeared when the antibody against SDF-1α was preincubated with excess of recombinant SDF-1α (2.5 μg) (Fig. 2*C*). Preincubation of the anti-NeuN antibody with 2.5 μg of SDF-1α had no effects on the signals yielded by NeuN

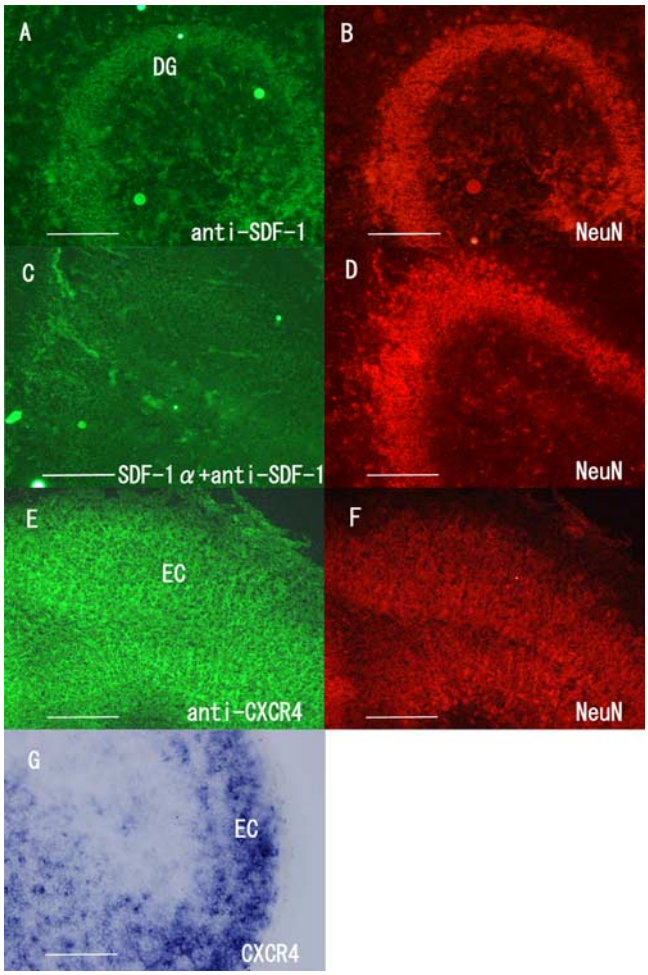

Figure 2. Distribution of stromal cell-derived factor 1α in the DG and of its receptor, CXCR4, in the EC. ***A***, ***B***, Axial sections of the DG obtained from rats at postnatal days 0–1 were immunostained with the anti-SDF-1α (***A***) and anti-NeuN antibodies (***B***). Double immunostaining with these antibodies demonstrated that SDF-1α is expressed in the granule neurons in the DG. ***C***, ***D***, A pilot experiment was performed to determine the specificity of the antibody to SDF-1α, and the absorption of the anti-SDF-1 antibody on preincubation with excess of SDF-1α was determined. ***C***, The immunoreactivity for SDF-1α in the DG disappeared. ***D***, The immunoreactivity for NeuN in the DG was maintained. ***E***, ***F***, Axial sections of the EC were stained with the anti-CXCR4 (***E***) and anti-NeuN antibodies (***F***). Double immunostaining with these antibodies demonstrated that CXCR4 is expressed in the EC neurons. ***G***, *In situ* hybridization for the detection of CXCR4 mRNA was performed in the axial section of the EC. Scale bars, 200 μm.

(Fig. 2*D*). Thus, the immunoreactivity for SDF-1α was proven to be specific.

Next, we assessed whether entorhinal neurons express the SDF-1α receptor. Immunohistochemical analysis was performed for axial sections of the EC by using the anti-CXCR4 and anti-NeuN antibodies. Colocalization of the immunoreactivity for CXCR4 and NeuN was observed in the EC cells (Fig. 2*E*,*F*). We performed *in situ* hybridization to confirm CXCR4 expression in the EC cells. The result demonstrated that CXCR4 mRNA expression was abundantly observed in the EC cells (Fig. 2*G*). Thus, CXCR4 is expressed in the EC. These results suggest that SDF-1α, which is expressed in the neurons in the DG, may act on entorhinal neurons expressing CXCR4.

SDF-1α promoted neurite growth in the dissociated entorhinal cortical neurons

Furthermore, we hypothesized that SDF-1α may play a role in the axonal elongation of entorhinal neurons. To assess this, we ex-

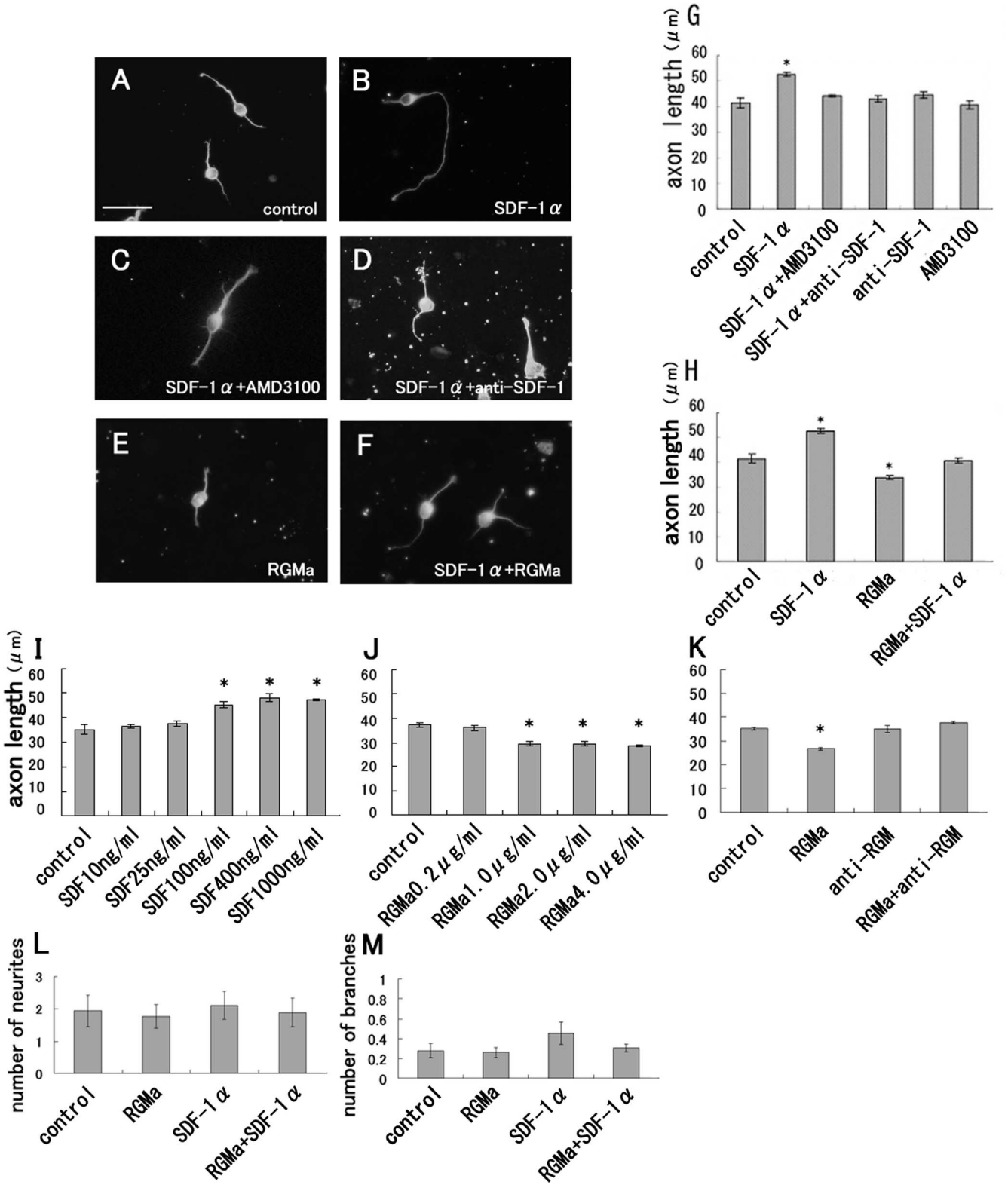

Figure 3. SDF-1α promotes neurite elongation in entorhinal cortical neurons *in vitro*. The EC neurons obtained from rats at postnatal day 0 were cultured in the absence (***A***) or presence of 400 ng/ml SDF-1α (***B–D***, ***F***). The neurons were stained with the mouse monoclonal anti-Tuj1 antibody. ***A***, ***B***, SDF-1α (400 ng/ml) promoted neurite growth in the EC neurons. ***C***, Coincubation with 400 ng/ml SDF-1α and 15 μg/ml AMD3100 (CXCR4 antagonist). ***D***, Coincubation with SDF-1α and 60 μg/ml anti-SDF-1 antibody. ***E***, RGMa (1 μg/ml) inhibited neurite growth. Scale bars, 25 μm. ***G***, Mean length of the longest neurite per neuron. AMD3100 as well as the anti-SDF-1 antibody abolished the effects of SDF-1α, although neither of these exerted any effects on neurite growth. ***H***, Coincubation with 1 μg/ml RGMa and 400 ng/ml SDF-1α resulted in the elimination of the effects of SDF-1α. The data are represented as the mean ± SEM of four independent experiments (***G***, ***H***). The asterisks (*) indicate statistical significance ($p < 0.05$) (one-way ANOVA followed by Scheffé's multiple-comparison test). ***I***, ***J***, The effects of SDF-1α (***I***) and RGMa (***J***) on neurite growth at the indicated concentrations. ***K***, The anti-RGMa antibody attenuated the neurite growth inhibition by RGMa. ***L***, The number of neurites per neuron. RGMa or SDF-1α does not alter the number of neurites significantly. ***M***, The number of branches per neuron. The data are represented as the mean ± SEM of four independent experiments (***I–M***). The asterisks (*) indicate statistical significance ($p < 0.01$) compared with the control (one-way ANOVA followed by Scheffé's multiple-comparison test).

amined the effects of SDF-1α on the neurite growth of entorhinal cortical neurons *in vitro*. The dissociated entorhinal cortical neurons isolated from rats at postnatal days 0–1 were either left untreated or treated with recombinant SDF-1α at a concentration of 400 ng/ml for 24 h, fixed, and immunostained with the TuJ1 antibody. The neurite length was then measured; the average neurite length was significantly greater in the SDF-1α-treated group than in the control group (Fig. 3*A*,*B*,*G*). Furthermore, to determine whether this effect of SDF-1α was dependent on SDF-1α and its receptor, CXCR4, we used AMD3100, which is a specific SDF-1 receptor antagonist, and a neutralizing antibody against SDF-1α. The effect of SDF-1α was completely abolished if the neurons were coincubated with AMD3100 (15 μg/ml) (Fig. 3*C*,*G*) or the anti-SDF-1 antibody (60 μg/ml) (Fig. 3*D*,*G*), although AMD3100 or the anti-SDF-1 antibody did not independently exert any modulating effects on neurite elongation (Fig. 3*G*). The neurite-promoting effect of SDF-1α was found at concentrations ranging from 100 to 1000 ng/ml (Fig. 3*I*). However, SDF-1α did not significantly change the number of neurites or branches per neuron (Fig. 3*L*,*M*). These results strongly suggest that SDF-1α promotes neurite growth in the entorhinal cortical neurons via its receptor CXCR4.

Stripe and outgrowth assays performed in a previous study revealed that entorhinal axons are repelled by RGMa (Brinks et al., 2004); this prompted us to examine the possible conflicting effects of SDF-1α and RGMa in our culture system. As expected, neurite growth in the entorhinal cortical neurons was significantly inhibited by RGMa (1–4 μg/ml) (Fig. 3*E*,*H*,*J*). The effects of SDF-1α (400 ng/ml) as well as RGMa (1 μg/ml) on neurite growth disappeared when the neurons were coincubated with both these molecules (Fig. 3*F*,*H*). In addition, the anti-RGM antibody neutralized the effect of the RGMa (Fig. 3*K*). These results support our notion that SDF-1α promotes, whereas RGMa inhibits, the neurite elongation of entorhinal neurons *in vitro*, which suggest the possibility that SDF-1α may be involved in navigating the entorhinal neurons toward the DG.

SDF-1α promotes neurite growth by a mechanism dependent on mDia1

We further explored the signaling pathway leading to the promotion of neurite growth by SDF-1α. It was previously demonstrated that mDia1 was involved in the signals downstream of SDF-1α, using cerebellar granule neurons (Arakawa et al., 2003). Thus, we assessed whether mDia1 was necessary for the effect of SDF-1α using the RNA interference technique. The entorhinal cortical neurons were transfected with mDia1 siRNA or the control siRNAs, and the expression of mDia1 was determined by Western blot analysis (Fig. 4*A*). The result demonstrated that mDia1 expression was decreased specifically at 1 or 2 d after the mDia1 siRNA transfection.

One day after the siRNA transfection, we treated the neurons with 400 ng/ml SDF-1α and incubated them for an additional 24 h. The neurite-promoting effect of SDF-1α was absent in the neurons transfected with mDia1 siRNA, but not with those transfected with the control siRNAs (Fig. 4*B*). However, Y-27632 (50 μM), the Rho kinase inhibitor, did not modulate the effect of SDF-1α (Fig. 4*B*). These results strongly suggest that SDF-1α promotes neurite growth by a mechanism dependent on mDia1.

SDF-1α navigates perforant fibers from the EC to the DG

Because the above results obtained from the *in vitro* analysis suggest that SDF-1α plays a role in navigation of the axons of the EC neurons to the DG, we attempted to test this hypothesis in a more

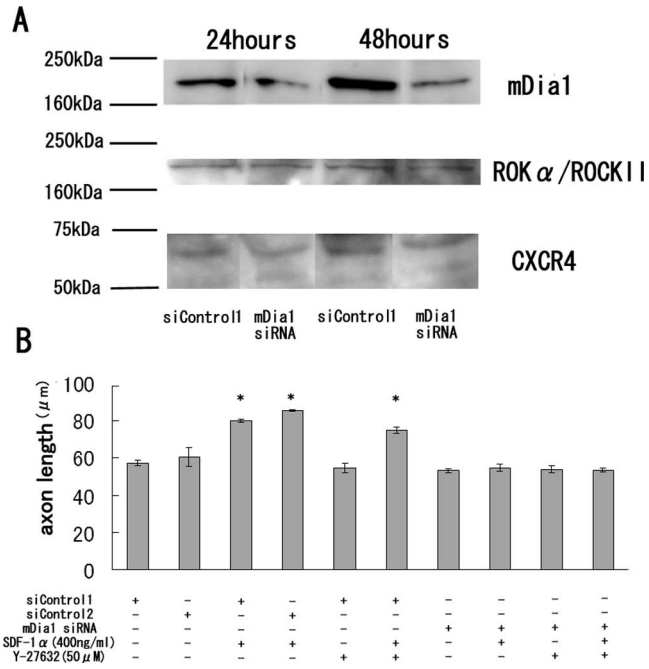

Figure 4. Neurite elongation by SDF-1α is dependent on mDia1. ***A***, The EC neurons obtained from rats at postnatal day 0 were transfected with mDia1 siRNA or control siRNA (si control). Western blot demonstrates reduction of mDia1 expression at 24 and 48 h by mDia1 siRNA. The expression of Rho kinase (ROKα) or CXCR4 was not changed by mDia1 siRNA. ***B***, Mean length of the longest neurite per neuron. The mDia1 knockdown resulted in inhibition of SDF-1α-dependent axon elongation. The data are represented as the mean ± SEM of four independent experiments. The asterisks (*) indicate statistical significance ($p < 0.05$) compared with the control (si control) (one-way ANOVA followed by Scheffé's multiple-comparison test).

direct manner. It has been reported that *CXCR4*-knock-out mice exhibit a defect in the migration of hippocampal dentate granule neurons during the embryonic stage (Bagri et al., 2002; Lu et al., 2002); thus, these mice were not appropriate for the purpose of our study. Therefore, to examine the effects of SDF-1α on axon projection from the EC to the DG, slices of the EC and hippocampus of rats at postnatal days 0–1 were cocultured. The EC specimens were obtained from GFP transgenic rats. An entorhinal cortical slice and a hippocampal slice were exactly placed to monitor the projection of the perforant fibers from the EC to the DG (Figs. 1, 5*A*), and the slices were incubated for 9 d in the absence or presence of 50 μg/ml AMD3100 or 60 μg/ml anti-SDF-1 antibody. As shown in Figure 5*A*, this coculture system facilitated distinct visualization of projection of the EC neuronal axons to the DG. The green fluorescent signals obtained in the DG reflected the fibers projecting from the EC (Fig. 5*A–C*), and these signals were specifically observed in the outer molecular layer of the DG. The green fluorescent intensities of the perforant fibers were measured and normalized to those obtained in the EC (Fig. 5*F*); the value thus obtained represented the level of neuronal projection from the EC to the DG. We then treated the explant culture with AMD3100 or the anti-SDF1 antibody. Notably, both treatments resulted in a significant reduction in the level of neuronal projection from the EC to the DG (Fig. 5*D–F*). However, this reduction was greater in the AMD3100-treated group than in the anti-SDF-1 antibody-treated group. These results suggest that SDF-1α and its receptor, CXCR4, are necessary for appropriate projection of the perforant fibers from the EC to the DG. However, because *CXCR4*-knock-out mice exhibit a defect in the migration of hippocampal dentate granule neurons during the embryonic stage, it is possible that treatment with the anti-SDF-1

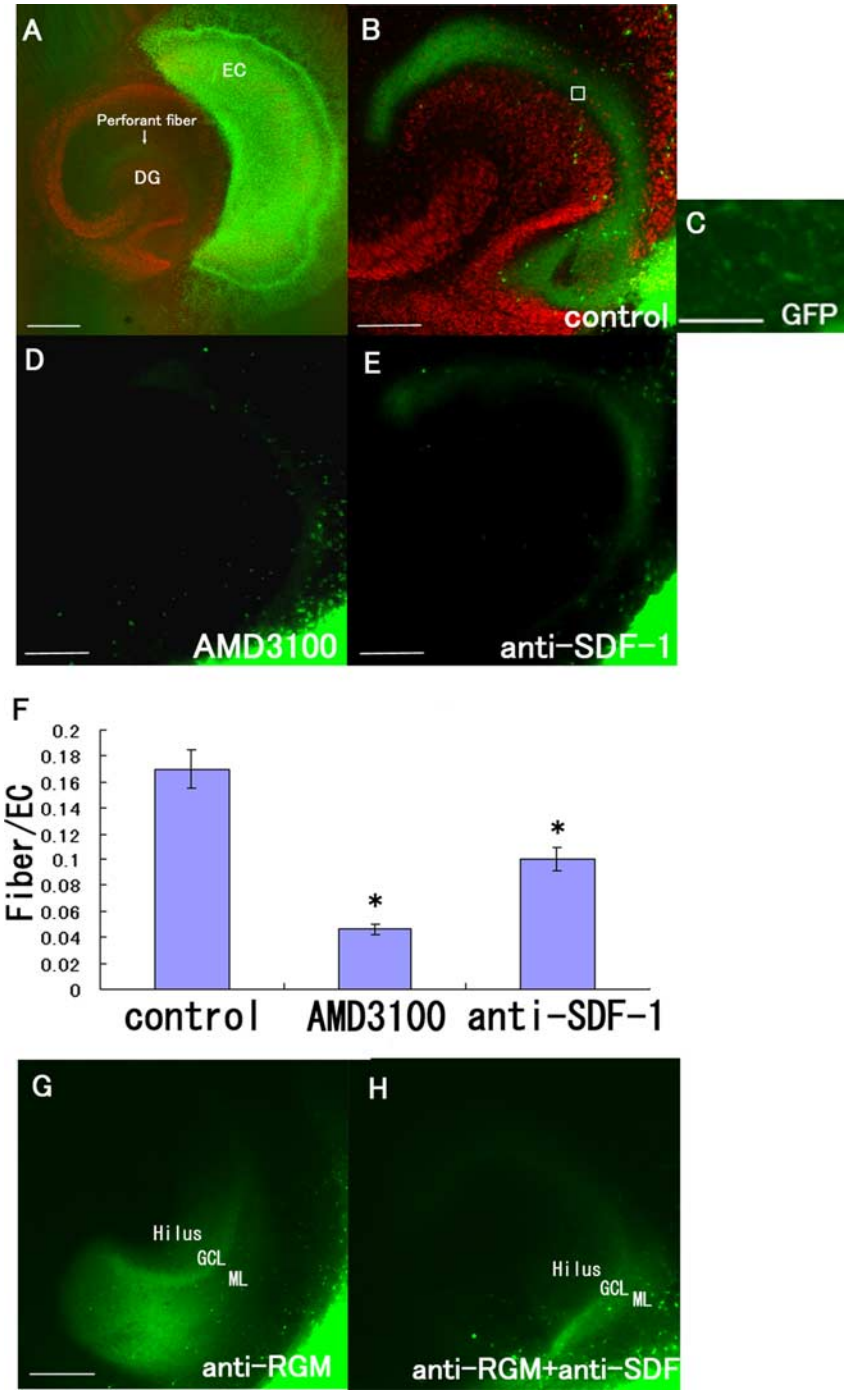

Figure 5. SDF-1α is necessary for the projection of perforant fibers from the EC to the DG. ***A***, The GFP-labeled EC (green) and DG (red; stained with anti-Prox1 antibody) slices were obtained from rats at postnatal days 0–1. ***B***, ***D***, ***E***, The tissue slices were incubated for 9 d in the absence (***B***) or presence of 50 μg/ml AMD3100 (CXCR4 antagonist) (***D***) or 60 μg/ml anti-SDF-1 antibody (***E***). ***A***, ***B***, Perforant fibers (arrow) running from the EC to the DG are visible. ***C***, High-magnification view of a square in ***B***. ***D***, ***E***, Treatment with AMD3100 (SDF-1 receptor antagonist) or the anti-SDF-1 antibody reduced the projection of the perforant fibers from the EC to the DG. ***F***, The fluorescence intensity of the perforant fibers in the DG was measured. The data are represented as the mean ± SEM of four samples (8 fields of 25 μm^2 each) of each group. The perforant fiber projection was significantly lower in the AMD3100- and anti-SDF-1 antibody-treated groups. The asterisks (*) indicate statistical significance ($p < 0.05$) (one-way ANOVA followed by Scheffé's multiple-comparison test). ***G***, ***H***, The tissue slices were incubated with anti-RGM antibody (***G***) or anti-RGM antibody and anti-SDF-1 antibody (***H***). Note the loss of the layer-specific termination of GFP-positive fibers after treatment with the anti-RGMa antibody. GCL, Granule cell layer; ML, molecular layer. Scale bars: ***A***, 500 μm; ***B***, ***D***, ***E***, ***G***, 200 μm; ***C***, 12 μm.

antibody or AMD3100 in our experimental model may have affected the migration of neurons to the DG, causing the projection of entorhinal neuronal axons to disappear. To rule out this possibility, we performed immunostaining by using the anti-Prox1 antibody, which is used for labeling dentate granule neurons (Fig. 6*A–C*). We observed that the DG structure was not disturbed after treatment with AMD3100 or the anti-SDF-1 antibody (Fig. 6*B*,*C*). Furthermore, no abnormal neuronal morphology was observed, and the number of neurons in the DG was not affected by these treatments (data not shown). These results demonstrate that blockade of the SDF-1–CXCR4 pathway for 9 d *in vitro*, beginning from postnatal days 0 and 1, does not disturb the DG structure. Thus, reduction in the perforant fiber projection on treatment with AMD3100 or the anti-SDF-1 antibody was not attributable to overall malformation of the dentate granule cell layers.

It was previously reported that disrupting the RGM function resulted in the loss of appropriate termination of the perforant fibers by using the coculture system (Brinks et al., 2004). We confirmed this result by using the neutralizing antibody to RGMa (Hata et al., 2006). After treatment with the anti-RGMa antibody, the perforant fiber projection was found diffusely in the DG (Fig. 5*G*), demonstrating inappropriate hippocampal projection. When we treated the coculture with the anti-RGMa and anti-SDF-1 antibodies simultaneously, signal intensity for the perforant fiber projection decreased compared with that of the anti-RGMa antibody treatment (Fig. 5*G*,*H*). This may be attributable to the combined effect of the loss of projection by the anti-SDF-1 antibody and inappropriate projection by the anti-RGMa antibody.

Appropriately projecting neurons form synapses with the target neurons; therefore, we assessed synapse formation between the perforant fibers and the dentate granule neurons. The hippocampal slices were cultured in contact with or in the absence of EC slices and were immunostained with the anti-PSD-95 antibody that labels postsynaptic densities on dendritic spines and with the anti-Prox1 antibody that labels granule cell layers (Fig. 7*A*,*B*). PSD-95-positive dots were observed in the border regions of the perforant fibers and the DG (Fig. 7*A*, square; *C*). The fluorescent dots labeled with the anti-PSD-95 antibody were counted in five different fields (each with a 100 μm^2 area) for each sample ($n = 4$), and the average number of dots was calculated (Fig. 7*G*). When the hippocampal slice was cultured in the absence of the EC slice, the number of PSD-95-positive dots (Fig. 7*D*,*G*) observed decreased considerably compared with the number observed when the control culture comprising the EC and DG was used (Fig. 7*C*,*G*). Thus, the re-

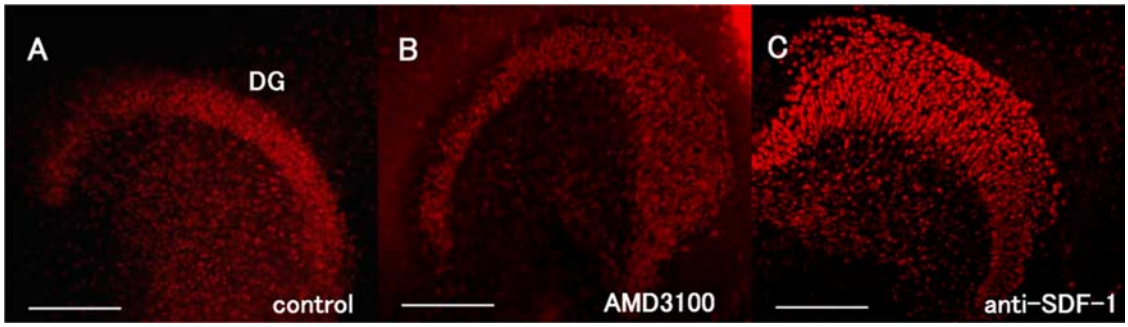

Figure 6. Treatment with AMD3100 or the anti-SDF-1 antibody does not disturb the DG structure. ***A–C***, Tissue slices of the EC and DG obtained from rats at postnatal days 0–1 were incubated for 9 d in the absence (***A***) (control) or presence of 50 μg/ml AMD3100 (***B***) or 60 μg/ml anti-SDF-1 antibody (***C***). The tissues were immunostained with the anti-Prox1 antibody. The structure of the dentate granule cell layers was maintained in all the groups. Thus, the reduced projection of the perforant fibers on treatment with AMD3100 or the anti-SDF-1 antibody was not attributable to the overall disturbance of the dentate granule cell layers. Scale bars, 200 μm.

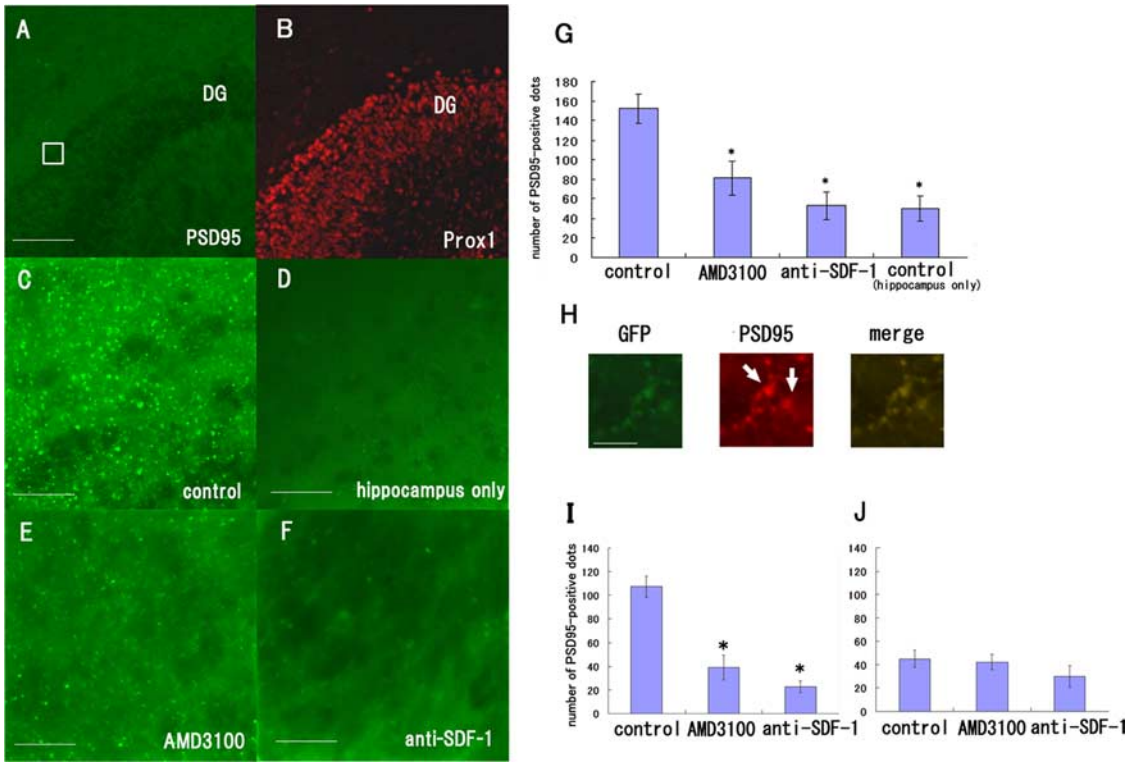

Figure 7. SDF-1α is necessary for synapse formation between the perforant fibers and the DG neurons. ***A***, Slices of the EC and hippocampus were obtained from the rats at postnatal days 0–1 and were incubated for 9 d in the absence (***A–C***) or presence of 50 μg/ml AMD3100 (***E***) or 60 μg/ml anti-SDF-1 antibody (***F***). ***D***, The hippocampal slices were cultured in the absence of the EC slices. The tissues were stained with the anti-PSD95 (green) and anti-Prox1 antibodies (red). ***C***, PSD-95-positive signals were observed between the perforant fibers and the DG. ***D***, The PSD-95-positive signals were considerably fewer in the hippocampal slices cultured in the absence of EC slices than in the coculture of the EC and hippocampus. ***E***, ***F***, Treatment with AMD3100 or the anti-SDF-1 antibody resulted in a decrease in the number of PSD-95-positive signals. ***G***, The number of PSD-95-positive signals in the DG was measured and quantified. ***H***, The hippocampal slices were obtained from wild-type rats and the EC slices were from GFP transgenic rats. The tissues were stained with the anti-PSD95 (red) and anti-GFP antibodies (green). The PSD-95-positive signals contacted with the GFP-positive perforant fibers. ***I***, The number of PSD-95-positive signals that contacted with the perforant fibers was measured and quantified. ***J***, The number of PSD-95-positive signals that did not contact with the perforant fibers was measured and quantified. ***G***, ***I***, ***J***, The data are represented as the mean ± SEM of four samples of each group (5 different fields of 100 μm^2 area for each sample). The asterisks (*) indicate statistical significance ($p < 0.05$) (two-way ANOVA followed by Scheffé's multiple-comparison test). Scale bars: ***A***, ***B***, 100 μm; ***C–F***, 25 μm; ***H***, 12 μm.

duced number of PSD-positive dots observed reflected synapses formed between the entorhinal and DG neurons. The PSD-95-positive dots observed in the case of the coculture of the hippocampal and EC slices treated with AMD3100 or the anti-SDF-1 antibody were significantly fewer than those observed in the case of the control group (Fig. 7*C*,*E–G*). To directly assess whether the decrease in synaptic density by the blockade of SDF-1 signaling is a consequence of reduction in the density of perforant fibers or a decrease in the density of synapses adjacent to perforant fibers, we performed simultaneous immunohistochemical analyses for PSD-95 and GFP. The PSD-95-positive dots contacted with the GFP-positive perforant fibers (Fig. 7*H*). We obtained consistent results when the number of PSD-95-positive dots contacted with the perforant fibers was counted (Fig. 7*I*). The number of the PSD-95-positive signals that did not contact with the perforant fibers was not significantly changed by either treatment (Fig. 7*J*). These results strongly support the notion that synapse formation between the perforant fibers and DG neurons depends on SDF-1α and its receptor.

Finally, we attempted to confirm that the perforant fibers pro-

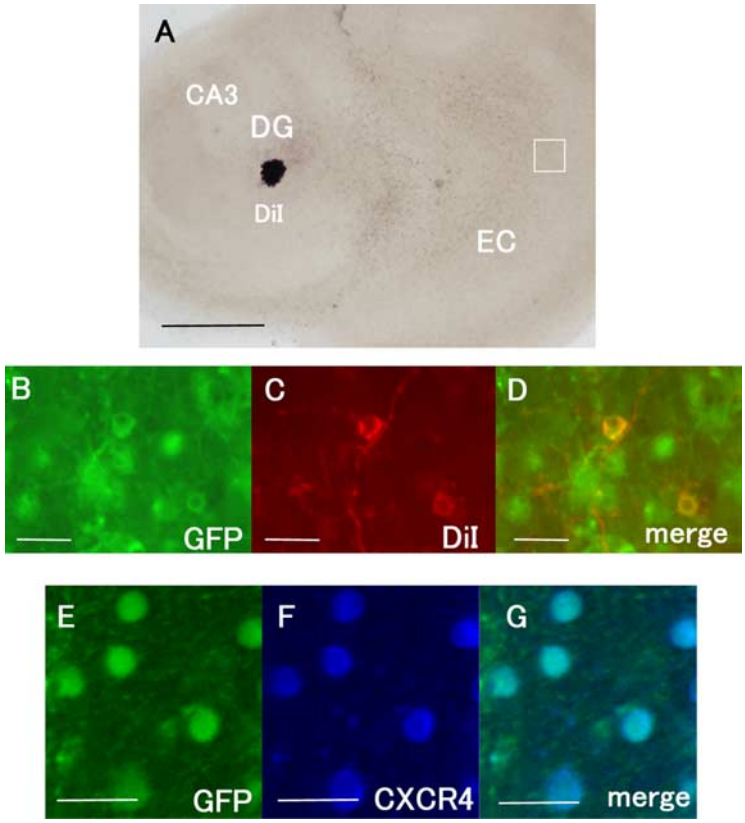

Figure 8. The EC neurons that project into the DG express CXCR4. ***A***, DiI was placed into the DG to label the perforant fibers. ***B–D***, The GFP signals in the EC were colocalized with those of DiI. ***E–G***, The immunoreactivity for CXCR4 (blue) is observed in the GFP-positive cells in the EC. Scale bars: ***A***, 500 μm; ***B–G***, 20 μm.

jecting to the DG expressed CXCR4. The cocultures were subjected to retrograde labeling of the perforant fibers projecting to the DG by DiI (Fig. 8*A*). The fibers and the neurons in the EC (Fig. 8*B–D*), which were labeled by DiI, were GFP-positive. The GFP-positive entorhinal neurons were immunoreactive for CXCR4 (Fig. 8*E–G*). Thus, these results demonstrate that the perforant fibers expressed the receptor for SDF-1α.

Discussion

The chemokine SDF-1α and its receptor, CXCR4, are known to play important roles in neural development (Tran and Miller, 2003). The present study unveiled several features of SDF-1α and CXCR4 during the early developmental stage of the hippocampus. First, the histochemical analysis revealed that SDF-1α is distributed in the DG neurons and that CXCR4 is expressed in the EC neurons of rats at postnatal day 0. Consistent with this observation, previous studies have reported that SDF-1α mRNAs are expressed in the granule cell layer of the DG in the brains of early postnatal rats (Tham et al., 2001; Berger et al., 2007). These data prompted us to hypothesize that SDF-1α expression in the DG induces axonal elongation of EC neurons expressing CXCR4.

SDF-1α promotes the neurite growth of dissociated EC neurons, and the neutralizing anti-SDF-1 antibody as well as AMD3100, a CXCR4 antagonist, abolishes this effect of SDF-1α. Because previous studies have demonstrated that SDF-1α promotes axonal elongation and the branching of hippocampal neurons (Arakawa et al., 2003; Pujol et al., 2005; Pritchett et al., 2007), SDF-1α distributed in the hippocampus may have multiple roles during neural development. Although, in the present study, the neurite growth assay for 24 h revealed that the number of branches or neurites was not significantly altered by SDF-1α, a longer assay time may be required to draw a conclusion. However, RGMa compels the entorhinal fibers to remain within their appropriate target zone (Brinks et al., 2004). Because our study shows that RGMa and SDF-1α exert opposing effects on the neurite growth of the EC neurons *in vitro*, conflicting signals elicited by these molecules are suggested to contribute to appropriate targeting of the perforant fibers. Thus, the ratio of the concentration of these factors in a local environment might determine the elongation, retraction, or termination of the perforant fibers. Interestingly, a previous report has demonstrated that SDF-1α reduces the repellent action of Slit-2 on retinal ganglion neurons; semaphorin 3A, on dorsal root ganglion neurons; and semaphorin 3C, on sympathetic neurons (Chalasani et al., 2003). However, these researchers did not observe the axon-promoting effects of SDF-1α on these neurons (retinal ganglion neurons, dorsal root ganglion sensory neurons, and sympathetic neurons) (Chalasani et al., 2003).

In the present study, we explored the signaling mechanism of axon elongation induced by SDF-1α. Facilitation of axon elongation of the cerebellar granule neurons by a low concentration of SDF-1α (100 and 250 ng/ml) was previously reported (Arakawa et al., 2003). This effect of axon elongation disappeared if the cells were treated with higher concentrations (500 and 1000 ng/ml) of SDF-1α (Arakawa et al., 2003), whereas our study revealed that SDF-1α at a concentration of 100–1000 ng/ml promoted neurite growth of the EC neurons. Consistent with the previous observation (Arakawa et al., 2003), the mDia1 pathway but not Rho kinase activation, is required for the promotion of neurite elongation in our study. Thus, our results support the critical role of the SDF-1α/mDia1 pathway in mediating axon elongation of the EC neurons.

The expression profiles of SDF-1α and CXCR4 and the axon-promoting effects of the former on dissociated entorhinal cortical neurons prompted us to assume that SDF-1α induces the projection of the perforant fibers from the EC to DG. However, because the structures of the DG as well as the cerebral cortex are destroyed in *CXCR4*-knock-out mice (Bagri et al., 2002; Lu et al., 2002; Paredes et al., 2006; Li et al., 2008), *CXCR4*- or *SDF-1*-knock-out mice were not appropriate for this analysis. To overcome this difficulty, we used entorhino-hippocampal slice cultures prepared from rats at postnatal days 0–1, in whom the dentate granule layers are almost established (Schlessinger et al., 1975; Altman and Bayer, 1990). A merit of this system is that the DG and cortical structures are not disturbed by blockade of the SDF-1–CXCR4 pathway. In addition, this coculture system enabled us to easily examine the molecular pathways by using specific inhibitors and neutralizing antibodies. With this slice culture system, we observed, for the first time, that blockade of the SDF-1–CXCR4 pathway reduced the projection of perforant fibers, as visualized via GFP signals; this strongly suggests that

SDF-1α promotes the growth of perforant fibers. Consistent with this observation, SDF-1α induces axonal elongation in cultured cerebellar granule neurons (Arakawa et al., 2003), and SDF-1α antagonizes the repellent effects of Slit/Robo signaling in the visual system (Chalasani et al., 2007). Therefore, it is suggested that SDF-1α is involved in promoting axonal growth in several types of neurons. Conversely, RGMa appears to restrict entorhinal fibers to their correct layer of the DG (Brinks et al., 2004). We confirmed this observation (Fig. 5*G*,*H*), and found that inhibition of both RGMa and SDF-1α resulted in reduction of the correct target axons from the EC. Therefore, SDF-1α and RGMa play important roles in correct navigation of the perforant fibers to the outer molecular layer of the DG. Concerning the signal transduction mechanism, we previously demonstrated that RGMa inhibits neurite growth by activating RhoA and Rho kinase (Hata et al., 2006). Because SDF-1α promotes neurite growth, which requires mDia1 (Fig. 4*B*), mDia1 and RhoA/Rho kinase pathways may be involved in appropriate termination of the perforant fibers, which requires elongation and termination of the axons.

PSD-95 belongs to a family of membrane-associated proteins found in the postsynaptic densities of neurons (Kornau et al., 1995; Nam and Chen, 2005). PSD-95 functions to recruit signaling components at the synapse (Kim and Sheng, 2004) and promotes the maturation of dendritic spines (El-Husseini et al., 2000; Charych et al., 2006). We detected PSD-95 immunoreactivity in the areas of contact between the dentate granule neurons and the perforant fibers. Because the number of PSD-95-positive particles on the perforant fibers was reduced when the SDF-1–CXCR4 pathway was blocked, this pathway may be associated with postsynaptic maturation of the perforant fibers and dentate granule neurons.

In conclusion, the present study identified a new molecule that promotes the axonal elongation of perforant fibers from the EC to the DG neurons. In the future, it would be interesting to determine whether a deficit in neural wiring can cause abnormal brain function.

References

Altman J, Bayer SA (1990) Migration and distribution of two populations of hippocampal granule cell precursors during the perinatal and postnatal periods. J Comp Neurol 301:365–381.

Ara T, Tokoyoda K, Okamoto R, Koni PA, Nagasawa T (2005) The role of CXCL12 in the organ-specific process of artery formation. Blood 105:3155–3161.

Arakawa Y, Bito H, Furuyashiki T, Tsuji T, Takemoto-Kimura S, Kimura K, Nozaki K, Hashimoto N, Narumiya S (2003) Control of axon elongation via an SDF-1alpha/Rho/mDia pathway in cultured cerebellar granule neurons. J Cell Biol 161:381–391.

Bagri A, Gurney T, He X, Zou YR, Littman DR, Tessier-Lavigne M, Pleasure SJ (2002) The chemokine SDF1 regulates migration of dentate granule cells. Development 129:4249–4260.

Belmadani A, Tran PB, Ren D, Assimacopoulos S, Grove EA, Miller RJ (2005) The chemokine stromal cell-derived factor-1 regulates the migration of sensory neuron progenitors. J Neurosci 25:3995–4003.

Berger O, Li G, Han SM, Paredes M, Pleasure SJ (2007) Expression of SDF-1 and CXCR4 during reorganization of the postnatal dentate gyrus. Dev Neurosci 29:48–58.

Bleul CC, Wu L, Hoxie JA, Springer TA, Mackay CR (1997) The HIV coreceptors CXCR4 and CCR5 are differentially expressed and regulated on human T lymphocytes. Proc Natl Acad Sci U S A 94:1925–1930.

Brinks H, Conrad S, Vogt J, Oldekamp J, Sierra A, Deitinghoff L, Bechmann I, Alvarez-Bolado G, Heimrich B, Monnier PP, Mueller BK, Skutella T (2004) The repulsive guidance molecule RGMa is involved in the formation of afferent connections in the dentate gyrus. J Neurosci 24:3862–3869.

Chalasani SH, Sabelko KA, Sunshine MJ, Littman DR, Raper JA (2003) A chemokine, SDF-1, reduces the effectiveness of multiple axonal repellents and is required for normal axon pathfinding. J Neurosci 23:1360–1371.

Chalasani SH, Sabol A, Xu H, Gyda MA, Rasband K, Granato M, Chien CB, Raper JA (2007) Stromal cell-derived factor-1 antagonizes slit/robo signaling *in vivo*. J Neurosci 27:973–980.

Charych EI, Akum BF, Goldberg JS, Jörnsten RJ, Rongo C, Zheng JQ, Firestein BL (2006) Activity-independent regulation of dendrite patterning by postsynaptic density protein PSD-95. J Neurosci 26:10164–10176.

Chen H, Bagri A, Zupicich JA, Zou Y, Stoeckli E, Pleasure SJ, Lowenstein DH, Skarnes WC, Chédotal A, Tessier-Lavigne M (2000) Neuropilin-2 regulates the development of selective cranial and sensory nerves and hippocampal mossy fiber projections. Neuron 25:43–56.

Cheng HJ, Bagri A, Yaron A, Stein E, Pleasure SJ, Tessier-Lavigne M (2001) Plexin-A3 mediates semaphorin signaling and regulates the development of hippocampal axonal projections. Neuron 32:249–263.

El-Husseini AE, Schnell E, Chetkovich DM, Nicoll RA, Bredt DS (2000) PSD-95 involvement in maturation of excitatory synapses. Science 290:1364–1368.

Gu C, Rodriguez ER, Reimert DV, Shu T, Fritzsch B, Richards LJ, Kolodkin AL, Ginty DD (2003) Neuropilin-1 conveys semaphorin and VEGF signaling during neural and cardiovascular development. Dev Cell 5:45–57.

Hata K, Fujitani M, Yasuda Y, Doya H, Saito T, Yamagishi S, Mueller BK, Yamashita T (2006) RGMa inhibition promotes axonal growth and recovery after spinal cord injury. J Cell Biol 173:47–58.

Kim E, Sheng M (2004) PDZ domain proteins of synapses. Nat Rev Neurosci 5:771–781.

Kornau HC, Schenker LT, Kennedy MB, Seeburg PH (1995) Domain interaction between NMDA receptor subunits and the postsynaptic density protein PSD-95. Science 269:1737–1740.

Koyama R, Yamada MK, Nishiyama N, Matsuki N, Ikegaya Y (2004a) Developmental switch in axon guidance modes of hippocampal mossy fibers *in vitro*. Dev Biol 267:29–42.

Koyama R, Yamada MK, Fujisawa S, Katoh-Semba R, Matsuki N, Ikegaya Y (2004b) Brain-derived neurotrophic factor induces hyperexcitable reentrant circuits in the dentate gyrus. J Neurosci 24:7215–7224.

Li G, Adesnik H, Li J, Long J, Nicoll RA, Rubenstein JL, Pleasure SJ (2008) Regional distribution of cortical interneurons and development of inhibitory tone are regulated by Cxcl12/Cxcr4 signaling. J Neurosci 28:1085–1098.

Lieberam I, Agalliu D, Nagasawa T, Ericson J, Jessell TM (2005) A Cxcl12-CXCR4 chemokine signaling pathway defines the initial trajectory of mammalian motor axons. Neuron 47:667–679.

Lu M, Grove EA, Miller RJ (2002) Abnormal development of the hippocampal dentate gyrus in mice lacking the CXCR4 chemokine receptor. Proc Natl Acad Sci U S A 99:7090–7095.

Ma Q, Jones D, Borghesani PR, Segal RA, Nagasawa T, Kishimoto T, Bronson RT, Springer TA (1998) Impaired B-lymphopoiesis, myelopoiesis, and derailed cerebellar neuron migration in CXCR4- and SDF-1-deficient mice. Proc Natl Acad Sci U S A 95:9448–9453.

Nam CI, Chen L (2005) Postsynaptic assembly induced by neurexin-neuroligin interaction and neurotransmitter. Proc Natl Acad Sci U S A 102:6137–6142.

Nguyen Ba-Charvet KT, Brose K, Marillat V, Kidd T, Goodman CS, Tessier-Lavigne M, Sotelo C, Chédotal A (1999) Slit2-Mediated chemorepulsion and collapse of developing forebrain axons. Neuron 22:463–473.

Okabe M, Ikawa M, Kominami K, Nakanishi T, Nishimune Y (1997) "Green mice" as a source of ubiquitous green cells. FEBS Lett 407:313–319.

Paredes MF, Li G, Berger O, Baraban SC, Pleasure SJ (2006) Stromal-derived factor-1 (CXCL12) regulates laminar position of Cajal-Retzius cells in normal and dysplastic brains. J Neurosci 26:9404–9412.

Pritchett J, Wright C, Zeef L, Nadarajah B (2007) Stromal derived factor-1 exerts differential regulation on distinct cortical cell populations in vitro. BMC Dev Biol 7:31.

Pujol F, Kitabgi P, Boudin H (2005) The chemokine SDF-1 differentially regulates axonal elongation and branching in hippocampal neurons. J Cell Sci 118:1071–1080.

Schlessinger AR, Cowan WM, Gottlieb DI (1975) An autoradiographic study of the time of origin and the pattern of granule cell migration in the dentate gyrus of the rat. J Comp Neurol 159:149–175.

Shimogori T, VanSant J, Paik E, Grove EA (2004) Members of the Wnt, Fz,

and Frp gene families expressed in postnatal mouse cerebral cortex. J Comp Neurol 473:496–510.

Skutella T, Nitsch R (2001) New molecules for hippocampal development. Trends Neurosci 24:107–113.

Stein E, Savaskan NE, Ninnemann O, Nitsch R, Zhou R, Skutella T (1999) A role for the Eph ligand ephrin-A3 in entorhino-hippocampal axon targeting. J Neurosci 19:8885–8893.

Steup A, Lohrum M, Hamscho N, Savaskan NE, Ninnemann O, Nitsch R, Fujisawa H, Püschel AW, Skutella T (2000) Sema3C and netrin-1 differentially affect axon growth in the hippocampal formation. Mol Cell Neurosci 15:141–155.

Stumm R, Höllt V (2007) CXC chemokine receptor 4 regulates neuronal migration and axonal pathfinding in the developing nervous system: implications for neuronal regeneration in the adult brain. J Mol Endocrinol 38:377–382.

Tham TN, Lazarini F, Franceschini IA, Lachapelle F, Amara A, Dubois-Dalcq M (2001) Developmental pattern of expression of the alpha chemokine stromal cell-derived factor 1 in the rat central nervous system. Eur J Neurosci 13:845–856.

Tran PB, Miller RJ (2003) Chemokine receptors in the brain: a developing story. J Comp Neurol 457:1–6.

Vilz TO, Moepps B, Engele J, Molly S, Littman DR, Schilling K (2005) The SDF-1/CXCR4 pathway and the development of the cerebellar system. Eur J Neurosci 22:1831–1839.

Zhao S, Förster E, Chai X, Frotscher M (2003) Different signals control laminar specificity of commissural and entorhinal fibers to the dentate gyrus. J Neurosci 23:7351–7357.

Zou YR, Kottmann AH, Kuroda M, Taniuchi I, Littman DR (1998) Function of the chemokine receptor CXCR4 in haematopoiesis and in cerebellar development. Nature 393:595–599.